15065 PORPHYRITIC SUBOPHITIC QUARTZ-NORMATIVE MARE BASALT ST. 1 1475.5 g

INTRODUCTION: 15065 is a coarse-grained quartz-normative basalt with pigeonite phenocrysts. It contains a pyroxene-rich segregation on one end. It is 3.3 b.y. old. It is blocky, subrounded (Fig. 1) and tough except on rounded surfaces. One end (laboratory W) is much more mafic than the rest of the rock and is a pyroxene accumulation--this portion is also more vuggy than the rest of the sample (Fig. 1). A few zap pits appear on most surfaces.

15065 was collected on the east flank of Elbow Crater, as one of several samples collected on a line extending out from the crater (Fig. 2). 15065 was closest to the crater, only 4 m east of the rim crest. The lunar orientation is known.

PETROLOGY: 15065 is a coarse-grained inequigranular basalt (often termed gabbro) with prismatic/euhedral pigeonite crystals which have greenish cores and red-brown rims. Most are 3 to 5 millimeters long. Plagioclases are white, anhedral to subhedral, and up to approximately 2.5 mm long.

15065 is a coarse member of the quartz-normative basalt group (e.g., Brown et al., 1972; Gay et al., 1972 and others), and is one of the most slowly-cooled members of that group. It is a little unusual for this group in containing a few percent magnesian olivine (Brown et al., 1972 and others) (Fig. 3d) and conspicuous tridymite laths (Fig. 3d, f). Published modes are listed in Table 1 (according to Juan et al., 1972 the sample contains nepheline but they have apparently misidentified tridymite). Fayalite is conspicuous with residual phases (tridymite, ulvospinel, etc.) in some sections, growing larger than 1 mm (Fig. 3d). In general the sample has been described as consisting of phenocrysts in a finer-grained groundmass of Ca-poor ferroaugite, calcic plagioclase, Fe-Ti oxides, minor sulfide and metal, prominent accessory apatite, and a residuum containing cristobalite and tridymite.

The few ragged anhedral Mg-olivines (Fo_{50-52}; Longhi et al. (1972) are enclosed by pyroxenes (Fig. 3d). Walker et al. (1977) record that grains of such olivine (which is unstable below 1100°C) are unzoned and homogeneous but each has a slightly different composition (Fo_{50-55}). The grains are large (~60 μm) and differ from liquidus olivines for this composition (Fo_{74}). The cooling rate was apparently slow enough to homogenize olivines by diffusion. The olivines produce some peculiar effects in crystallization experiments (see Walker et al. 1977).

The pyroxenes are composite, complexly zoned, and twinned (Fig. 3); some are hollow crystals (Fig. 3c). Some are complexly intergrown with plagioclase (Fig. 3b), with patches of pyroxene appearing to be poikilitically enclosed in plagioclase but optically continuous with larger pyroxenes. According to Longhi et al. (1972) this texture results

from slow late-stage crystallization of these two phases. Details of pyroxene compositions are given by Grove and Bence (1977) (Fig. 4), in a study aimed at assessing cooling rates (below). Yajima and Hafner (1974) used x-ray diffraction and Mossbauer techniques to find the distribution of Fe^{2+} and Mg^{2+} over the M, and M_2 sites, finding a distribution corresponding to equilibration close to 600°C; they also provided microprobe analyses of pyroxenes. They found no trace of exsolved augite or of cation distribution resulting from shock. Nakazawa and Hafner (1976) noted that the precession plots of Yajima and Hafner (1974), while not showing high-temperature exsolution, do show a small amount of low temperature augite exsolution. Jedwab (1972) described microvugs in pyroxenes as characterized with SEM, EMP, and photon microscope techniques. The vugs are complex and zonally arranged and contain small opaques and/or K-feldspar. Juan et al. (1972) reported 2v data for pyroxenes: 90° in the core pigeonites and 30° in subcalcic augite rims.

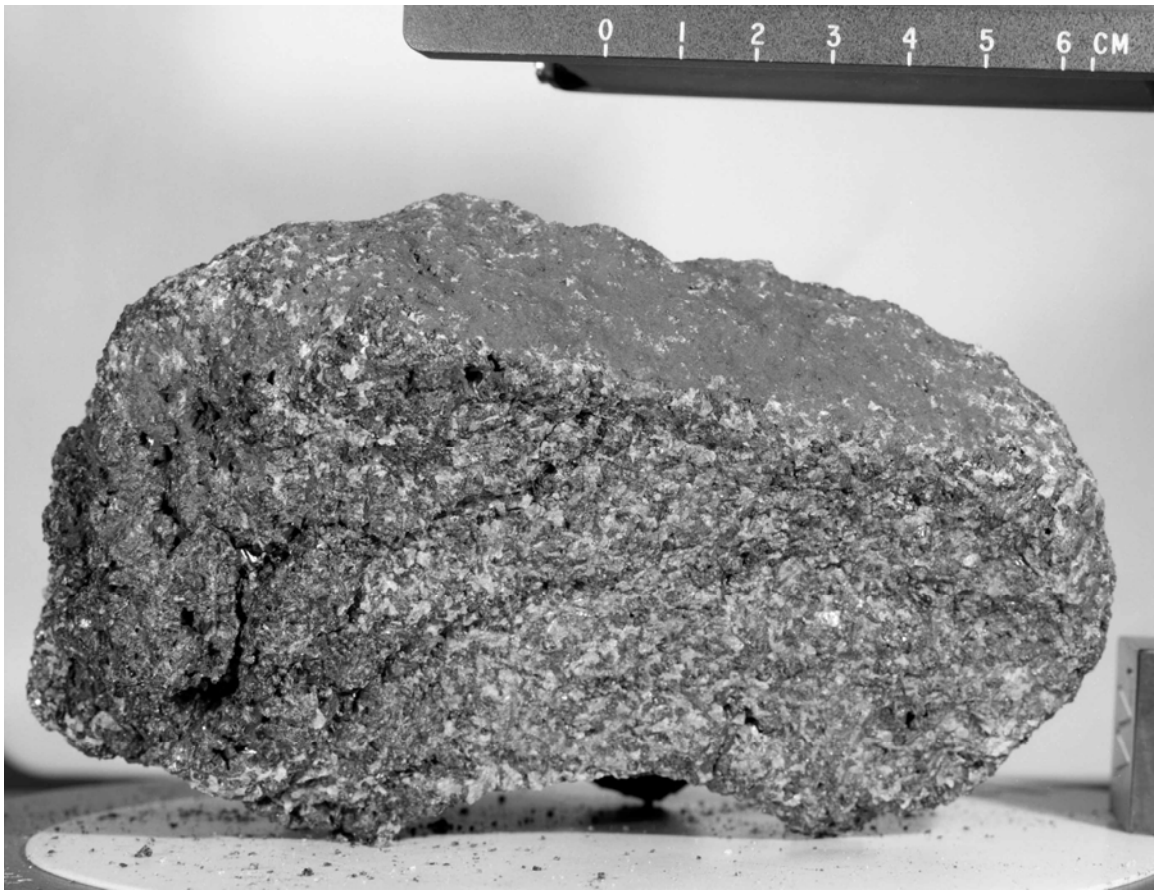

Figure 1. Pre-split picture of 15065, showing vuggy mafic segregation on B/W end (left), and normal coarse texture. S-71-45638

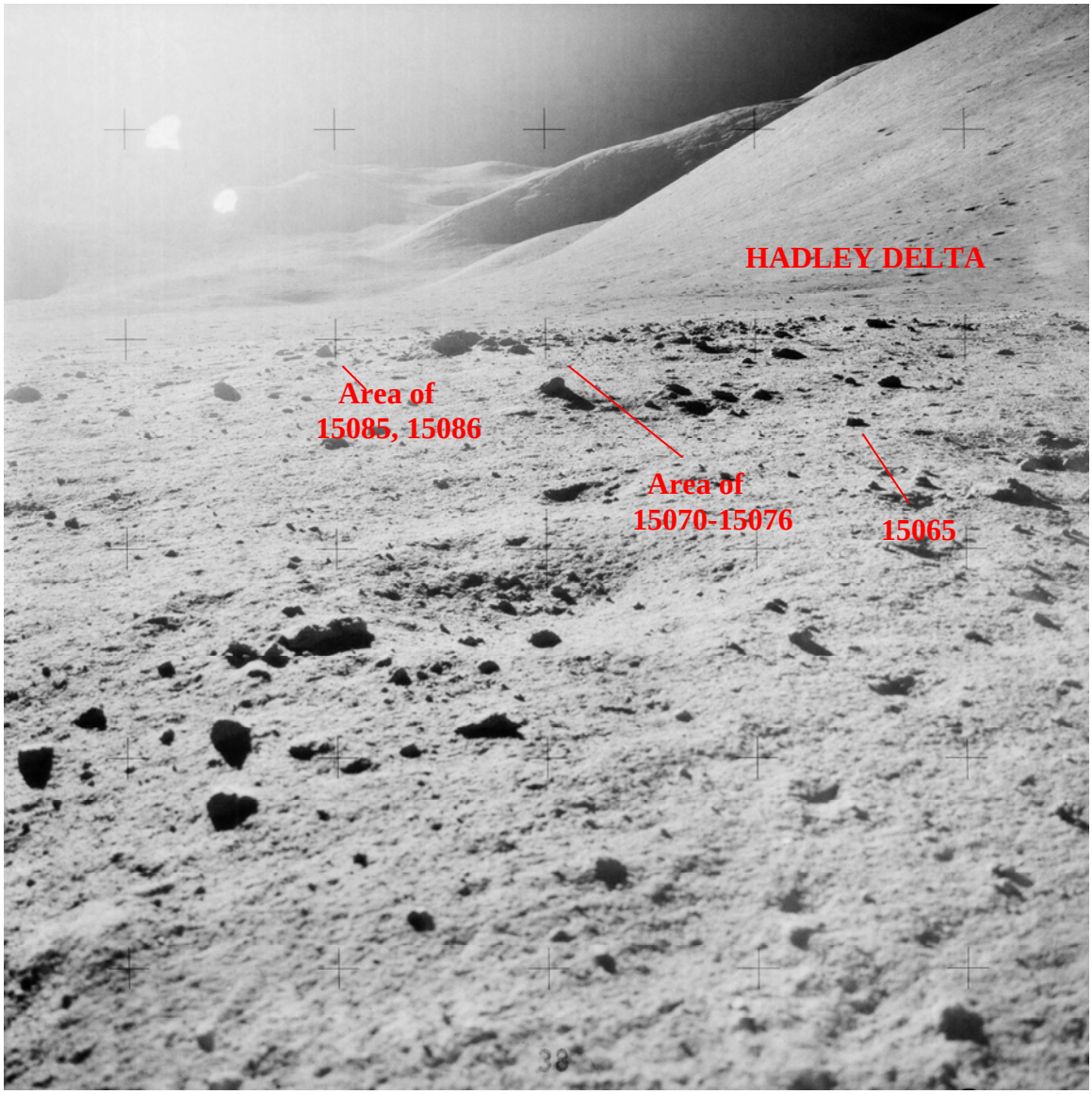

Figure 2. Sampling location of 15065 near the Elbow Crater rim. AS-15-11408

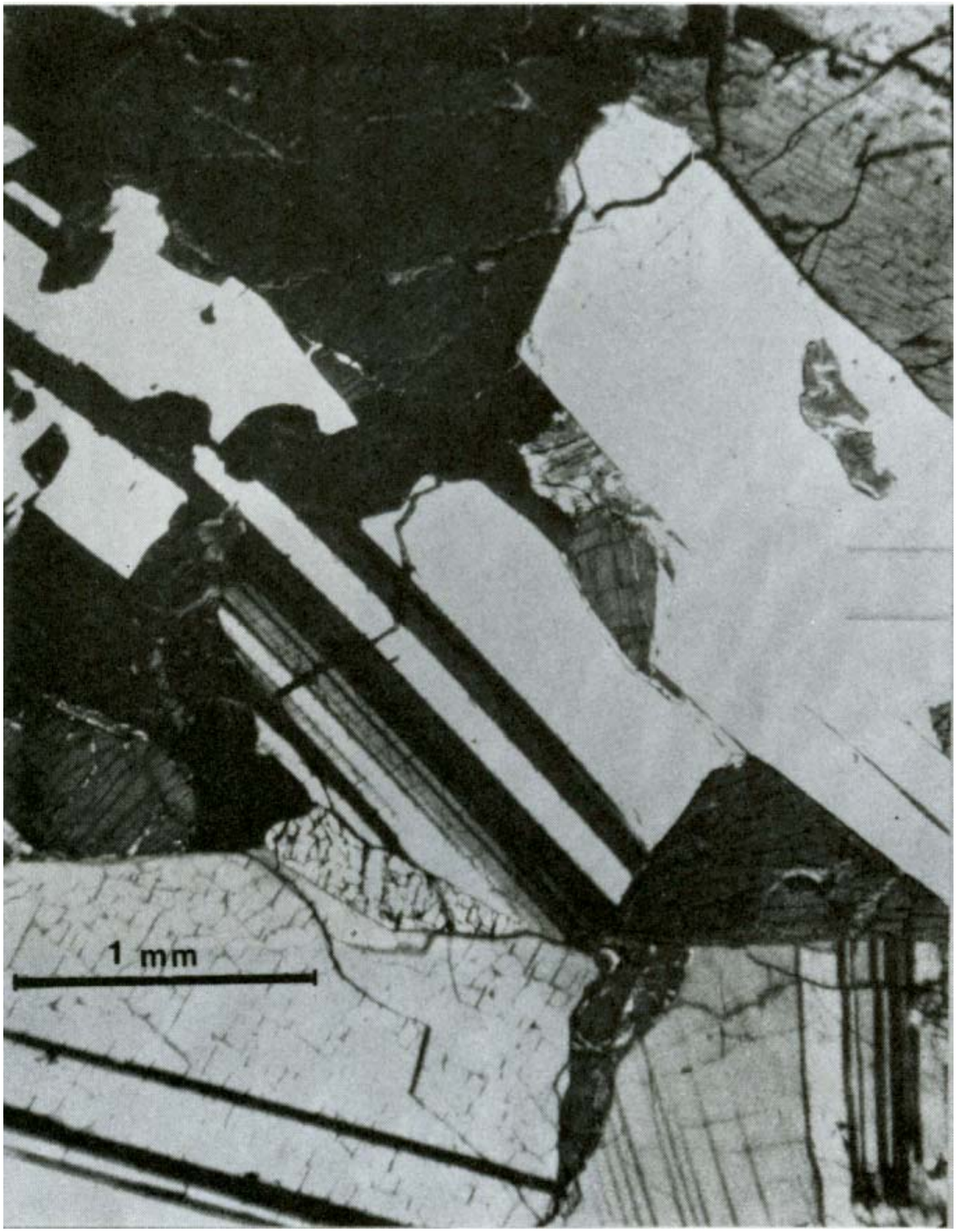

Fig 3a

Fig. 3b

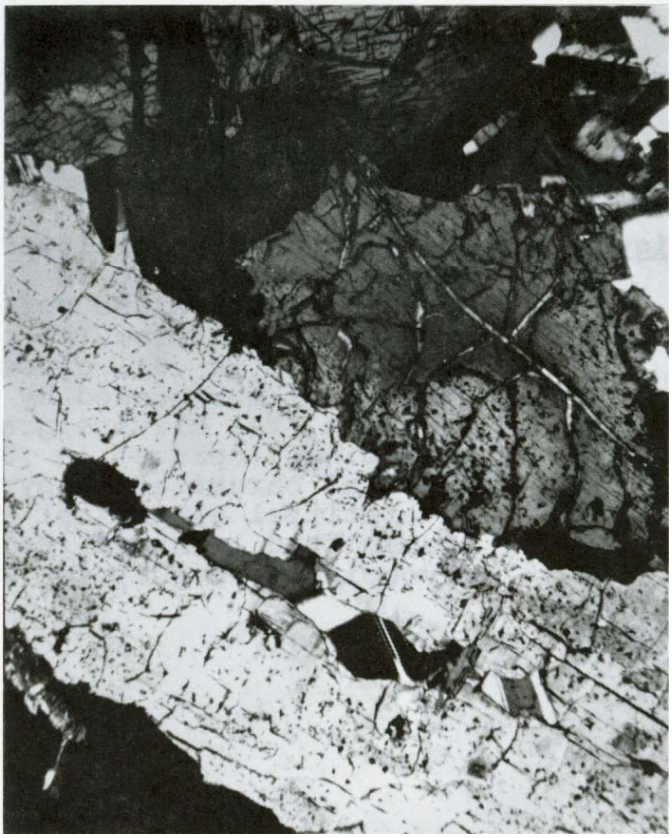

Fig. 3c

Fig. 3d

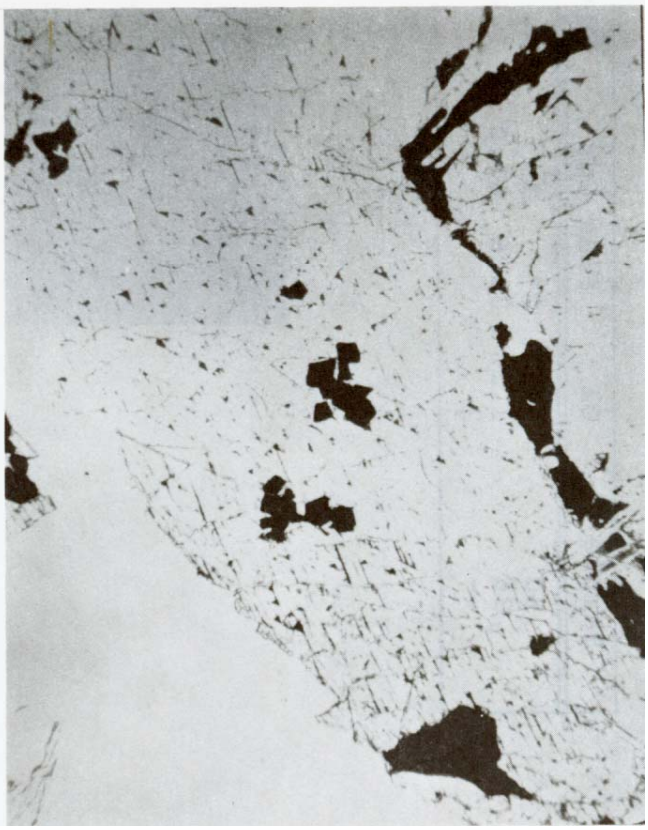

Fig. 3e

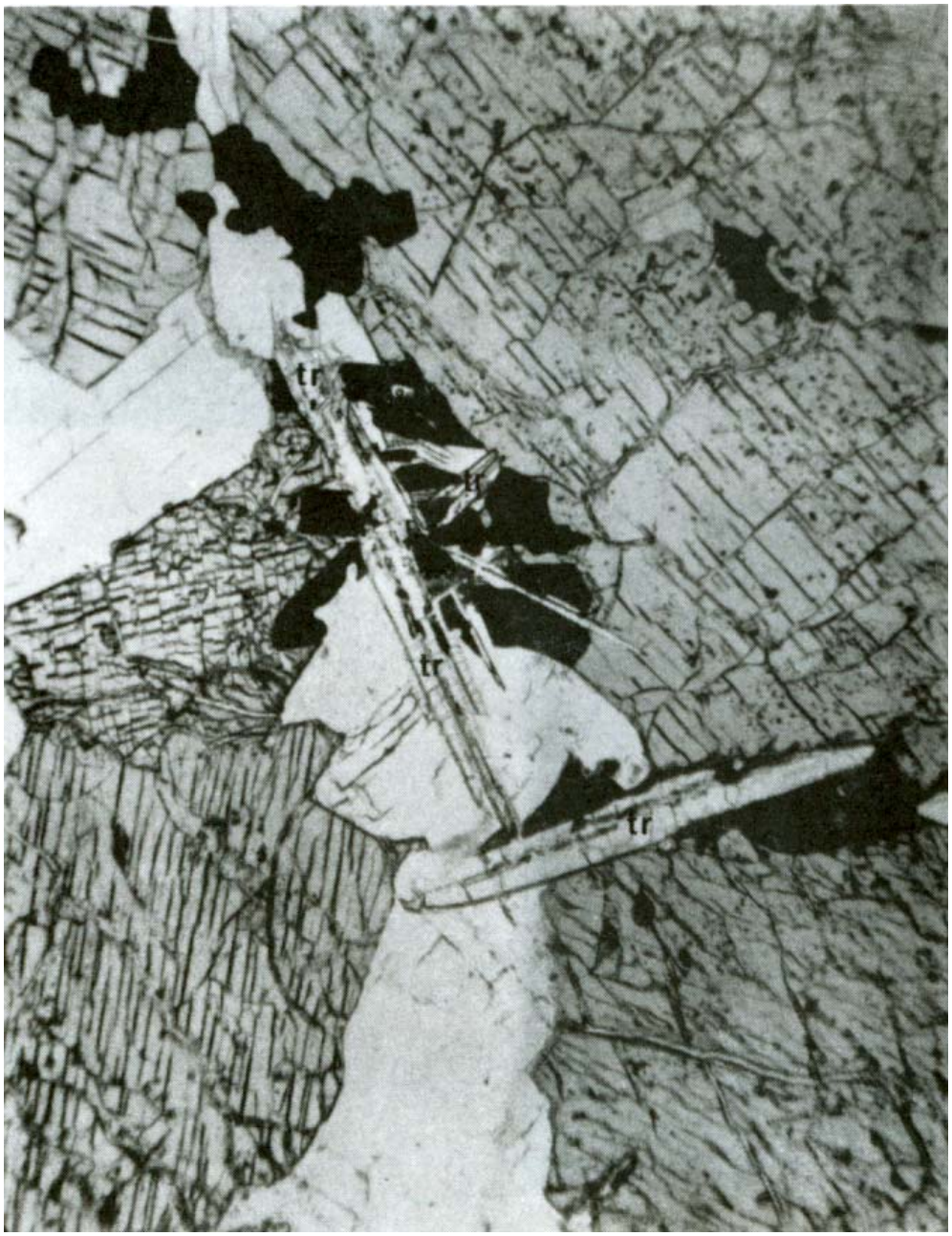

Fig. 3f

Figure 3. Photomicrographs of 15065 all to same scale.
(a) Gabbroic aspect in ,90, crossed polarizers;
(b) pyroxene plagioclase complex intergrowth in ,74, crossed polarizers;
(c) pyroxene phenocrysts showing hollow core in ,91, crossed polarizers;
(d) Mg-olivine cores (fo) surrounded by pyroxene and residual fayalite (fa) olivine grain tridymite (tr) and ulvospinel (opaque) in ,81, crossed polarizers;
(e) euhedral chromites in pyroxene core, with anhedral interstitial ulvospinel and ilmenite in ,90, plane transmitted light
(f) tridymite (tr) laths with ulvospinel (opaque) in ,81, transmitted light.

TABLE 15065-1. Published modes of 15065

Sample	Ol	Plag	Cpx	Gl+Sil	Opaques	Reference
,90	--	27	70	--	2	Juan et al.(1972)
,86	1.3	31.6	63.0	1.9	2.2	Longhi et al. (1972
--	2					Brown et al. (1972)

Most plagioclases are anhedral and they are often complexly twinned. They are zoned and often enclose pyroxenes poikilitically. According to Longhi et al.(1972) they are zoned from An_{91} to An_{80} , while Juan et al. (1972) merely reported a single value of An_{77}. Longhi et al. (1976) plotted An vs. Fe (Fe+Mg) of plagioclase crystals (Fig. 5), demonstrating a positive correlation of iron and sodium. Juan et al. (1972) stated that plagioclase probably crystallized earlier than clinopyroxene but with some coprecipitation; however this is in contrast with textural observations and experimental data which indicate that plagioclase crystallized later than pyroxene.

El Goresy et al. (1976) noted that 15065 and other coarse basalts contain corroded and rounded chromite cores as inclusions in Cr-ulvospinel, while idiomorphic Ti-chromites without any sign of optical zoning are included in olivine. The earliest chromite crystallized before plagioclase, probably before pyroxenes, and before or during olivine crystallization. El Goresy et al. (1976) diagrammed the zoning trends (Fig. 6a) and discussed the substitutions involved. Taylor et al. (1975) also analyzed spinels (Fig. 6b). Taylor and McCallister (1972a,b), Taylor et al. (1973, 1975), and Onorato et al. (1979) discussed the partitioning of Zr between ilmenite and ulvospinel, and the subsolidus reduction of ulvospinel to ilmenite and Fe-metal, as informants on cooling rates (below). Taylor et al. (1975) also analyzed Fe, metal compositions (Fig. 7). Jedwab (1972) described the iron as facetted and isometric, and probably of late crystallization. He also reported Ca-Fe phosphate deposited as hexagonal plates on a face-growing ilmenite crystal. Wark et al. (1973) presented an analysis of zirconolite, and Blank et al. (1982) used a proton probe to analyze for Zr and Nb in ilmenite/spinel pairs; they found ~200 ppm Zr in chromite, ~1000 ppm in ulvospinel, and ~10,000 ppm in ilmenite (Fig. 8).

Cooling rates: Lofgren et al. (1975), in a comparison of the products of linear cooling rate dynamic experiments with the natural rock, deduced a cooling rate of less than 1°C/hr from both the pyroxene phenocryst shapes and the "groundmass" textures for 15065, making it one of the slowest-cooled of the quartz-normative basalts. In a more detailed but similar type of analysis, Grove and Walker (1977) deduced cooling rates of 0.03°C to 0.1°C/hr at first (from pyroxene nucleation density), and a late stage cooling rate of 0.01°C/hr (from plagioclase "size"). The pyroxenes were larger than any produced in experiments cooled at 0.5°C/hr. The results are consistent with a slow, nearly linear cooling rate and suggest a distance of 1032 cm from a conductive boundary. The chemistry of the pyroxene cores is similar to those of equilibrium experiments (Grove and Bence, 1977). Walker et al. (1.977) concluded that the similarity of natural cores with experimental products precluded the presence of any significant cumulus pyroxene, and that the sample was not supercooled at pyroxene entry. Neither is the olivine (very little, and more Fe-rich than liquidus olivines) a possible cumulus phase.

The cooling rates were slow enough to homogenize olivine (but not pyroxene); modeling olivine diffusion produces a cooling rate of 0.3°C/day. The 15065 magma body must have taken a year or two to traverse the solidification interval.

Taylor and McCallister (1972a,b), Taylor et al. (1973, 1976), and Onorato et al. (1979) used the distribution of Zr between ulvospinel and ilmenite to deduce equilibration temperatures (~850°C) and cooling rates (~0.15°C to 1.0°C/day), consistent with other data showing lower cooling rates and equilibration temperatures than most other quartz-normative basalts. Brett (1975) used available kinetic data to deduce crystallization ~2 m from a boundary.

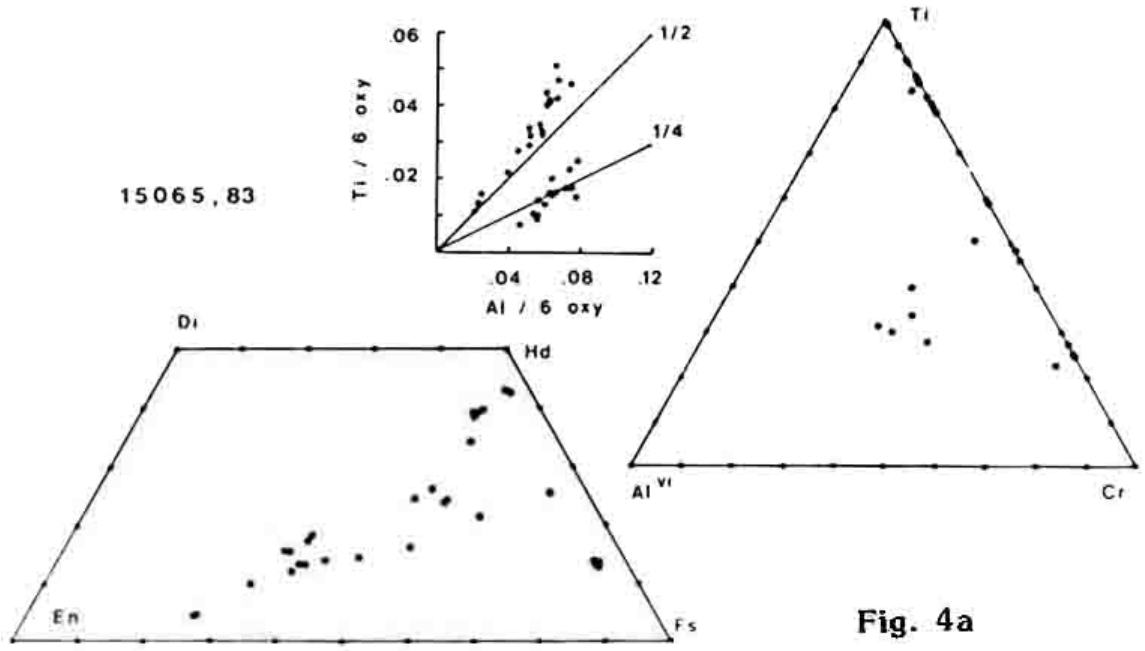

Fig. 4a

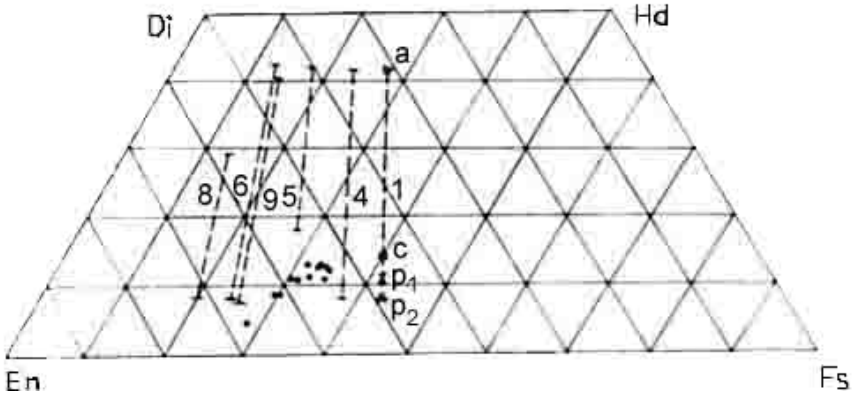

Fig. 4b

Figure 4. Pyroxene compositions.
a) Grove and Bence (1977); b) Yajima and Hafner (1974).

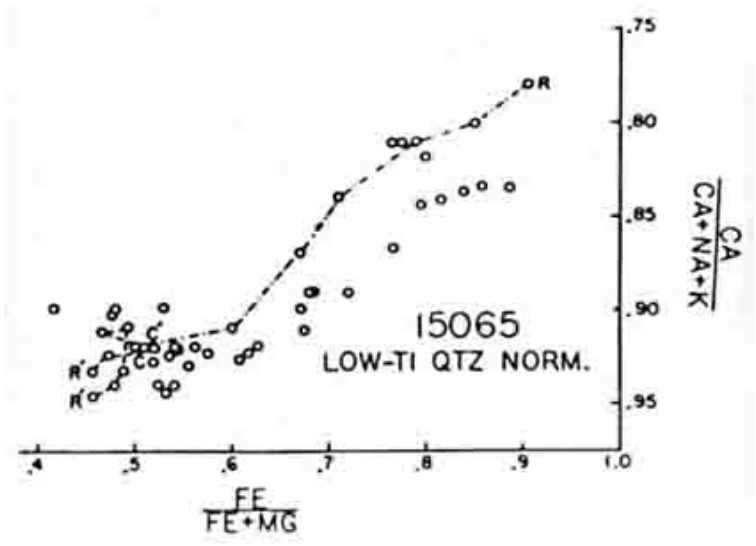

Figure 5. Plagioclase compositions
(Longhi et al.,1976).

EXPERIMENTAL PETROLOGY: Longhi et al. (1972) conducted equilibrium crystallization experiments on a 15065 rock powder, from low pressure to 20 kb (Fig. 9). The low pressure crystallization sequence is similar to that inferred from the natural rock, but the late-stage phases were not crystallized.

Fe-loss is a problem (see discussion of 15065 experiments in O'Hara and Humphries, 1977) making liquidus mafics too magnesian; even so Longhi et al. (1972) concluded that cumulus pyroxene was probably present.

Walker et al. (1977) conducted detailed experiments on 15065 natural powders in attempts to determine the optimum experimental conditions and containers. They reported results for low pressure (various containers) and for pressures up to 30 kb (molybdenum containers). Neglecting spinel, whose crystallization is enhanced in molybdenum containers, clinopyroxene is the liquidus phase at elevated pressures; there is a problem with reproducibility in these high pressure, near-solidus experiments.

Longhi et al. (1978) used the 15065 composition in studying olivine-liquid distribution coefficients for iron and magnesium, providing analyses of one olivine-liquid pair for a low pressure experiment at 1249°C. All other experiments (Lofgren et al., 1976; Grove and Bence, 1977) were dynamic experiments on an analog composition, not precisely 15065.

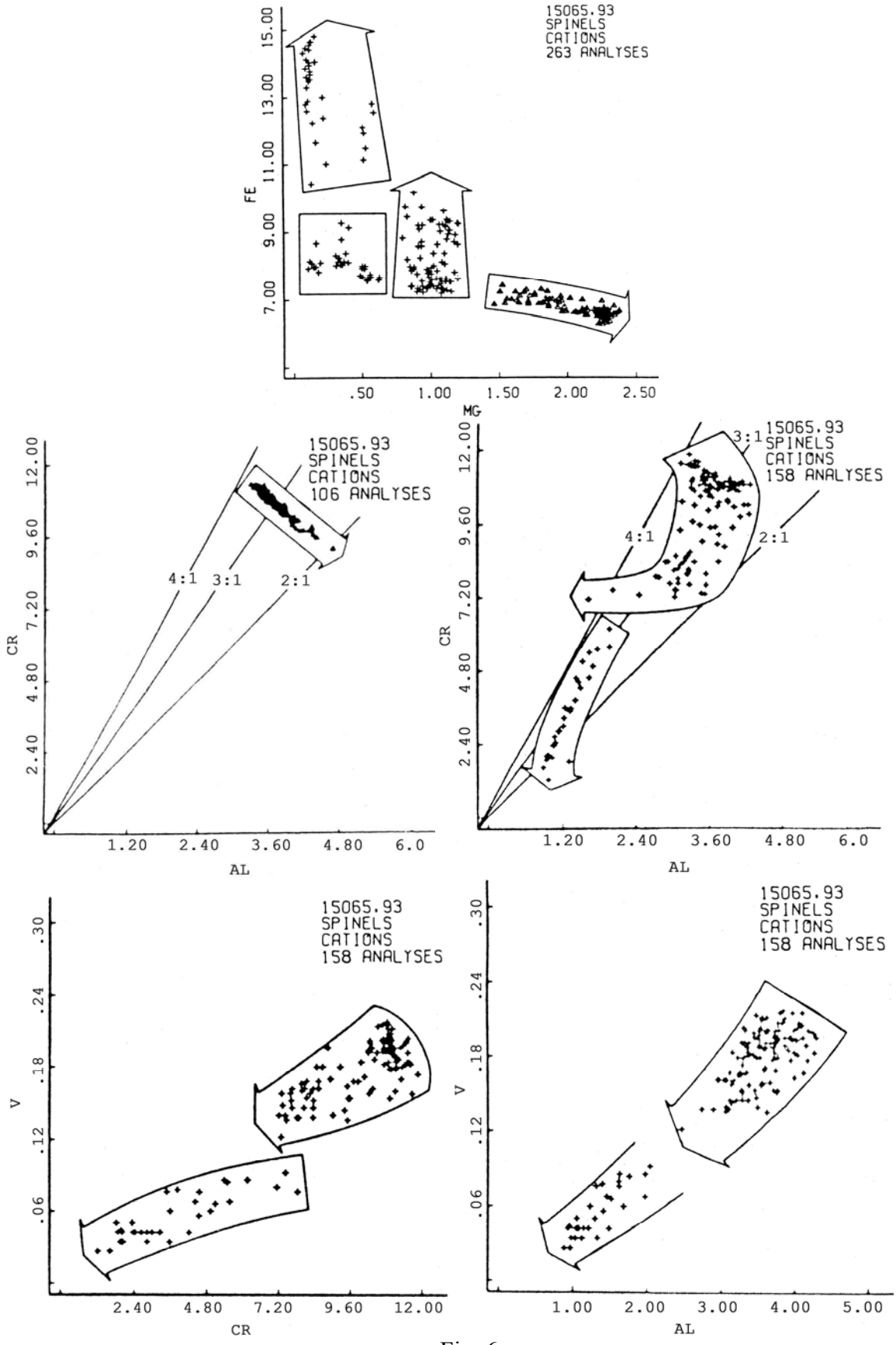
15065.93
SPINELS
CATIONS
263 ANALYSES
FE
MG
15065.93
SPINELS
CATIONS
106 ANALYSES
4:1
3:1
2:1
CR
AL
15065.93
SPINELS
CATIONS
158 ANALYSES
4:1
3:1
2:1
CR
AL
15065.93
SPINELS
CATIONS
158 ANALYSES
V
CR
15065.93
SPINELS
CATIONS
158 ANALYSES
V
AL

Fig. 6a

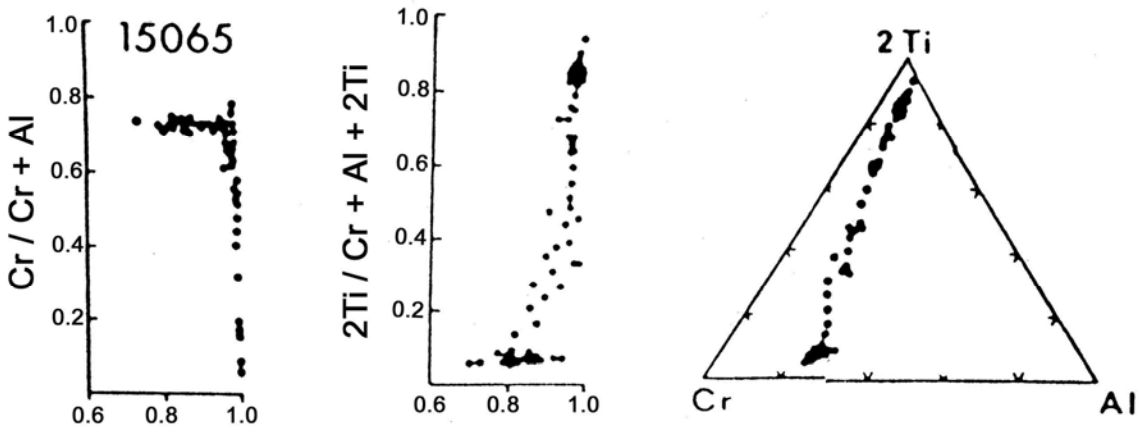

Fig. 6b

Figure 6. Spinel compositions.
a) El Goresy et al. (1976); b) Taylor et al. (1975).

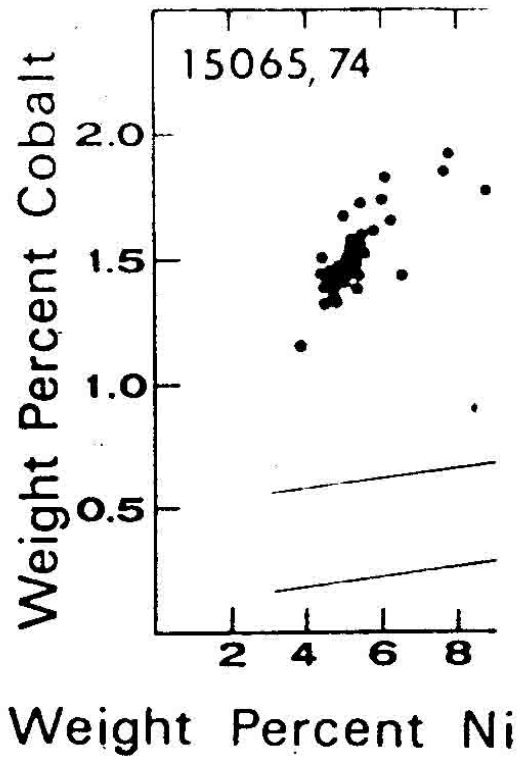

Figure 7. Fe-metal compositions (Taylor et al., 1975).

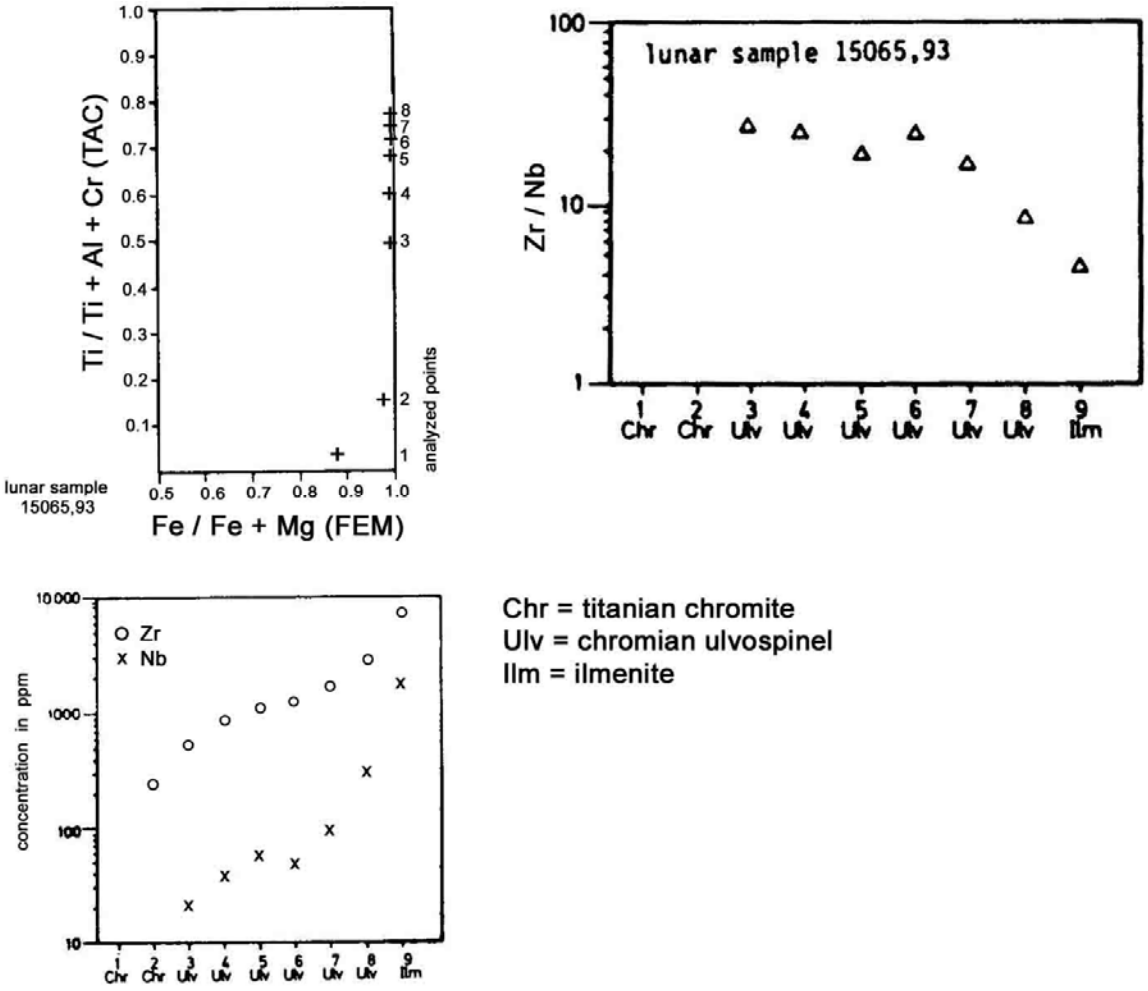

Figure 8. Zr abundances in opaque phases (Blank et al., 1982).

CHEMISTRY: The published chemical data are separated into "normal" rock (Table 2) and mafic segregation (Table 3) according to the split location. Rare earths are shown on Figure 10. If the limited data of Christian et al. (1972)/Cuttitta et al. (1973) are credible, then the mafic segregation is richer in rare earths than "normal" rock. The mafic segregation is certainly richer in K_2O and P_2O_5, it is also vuggier (macroscopic observations), and contains more conspicuous tridymite and fayalite (microscopic observation). One "normal" rock analysis seems wholly inconsistent: that of Juan et al., which is low in silica, high in CaO and Na_2O, and produces normative nepheline as well as 30% normative olivine. Otherwise the "normal" rock is fairly similar to other Apollo 15 quartz-normative basalts, but is more magnesian. Rhodes and Hubbard (1973) found that its composition could not be derived from other members of the group by additions or removal of potential low-pressure liquidus phases. Hence it actually represents a

separate magma type or unusual crystallization processes. One other inconsistency is that Ganapathy et al. (1973) refer to ,41, not ,5, as their mafic split (also in Wolf and Anders, 1980), in contradiction to the allocation records. Their analysis of ,5, allocated as mafic, has higher Rb, Cs, and U than ,41, consistent with the higher rare earths, K_2O, and P_2O_5 of the other mafic splits.

Cuttitta et al. (1973) analyzed for Fe_2O_3, finding none, and found an excess reducing capacity for ,31 ("normal") not present in ,8 (mafic). They ascribe the 64 ppm Cu in ,31 and the 32 ppb B in ,8 to probable contamination in the lunar laboratory. Gibson and Moore (1972) studied inorganic gas releases of the sample on heating, noting an absence of solar-wind derived species such as H_2 and CO_2. The sample has lower abundances of volatiles than do soils, by a factor of 5 to 10. Bibring et al. (1974) studied carbon extracted by vacuum sublimation from a crushed internal piece in efforts to understand lunar carbon chemistry. Gibson et al.(1975) analyzed for CO, CO_2, H_2, H_2S , Fe^0 with combustion, hydrolysis, and magnetic techniques. Wanke et al. (1975) also specifically analyzed for oxygen. Gibson and Andrawes (1978) found very low upper limits for H_2, CN_4, Ar, CO, acid CO_2, finding the absence of C-containing gases to be surprising.

In their discussion of the chemistry of Apollo 15 basalts, Pratt et al. (1977) did not seem to be aware of the mafic segregation specifically sampled in 15065, noting only gross compositional heterogeneities.

Barker (1974) attempted to find the composition of gases in the 15065 magma, by attempting to analyze the gases in glass inclusions in 15065,44. The sample was heated and gases measured with mass spectrometry. Barker (1974) diagrammed the evolution of H_2O, CO_2, and CO as a function of temperature. He concluded that the gas in the parent magma started with a composition close to 46% O, 42% C, and 12% H, and became more H_2O-rich as crystallization progressed. This result is in contradiction with the general conclusion that lunar basalts are and were devoid of water.

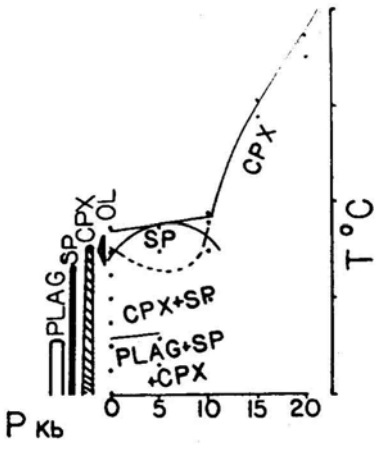

Figure 9. Phase relationships (Longhi et al., 1972).

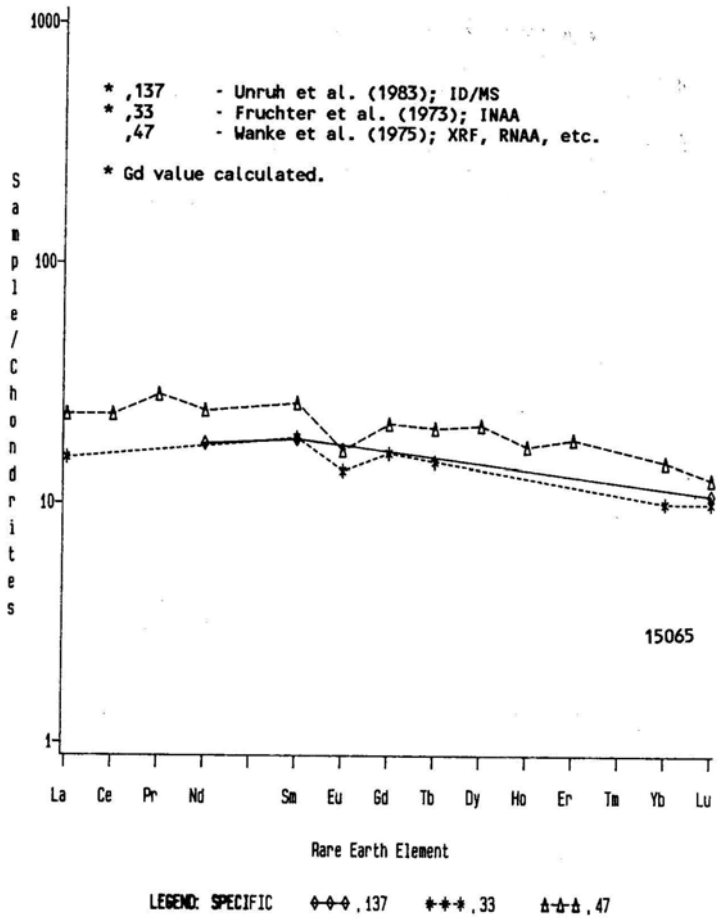

Figure 10. Rare earths

STABLE ISOTOPES: Clayton et al. (1973) reported oxygen isotope analyses for mineral separates from "normal" 15065 (Table 4), finding the fractionations consistent with typical magmatic temperatures of equilibration, i.e., ~1100°C. Strasheim et al. (1972) reported a $^{7}Li/^{6}Li$ ratio of 13.5, also for a "normal" sample.

RADIOGENIC ISOTOPES AND GEOCHRONOLOGY: Papanastassiou and Wasserburg (1973) determined a Rb-Sr internal isochron age of 3.28 ± 0.04 b.y. ($\lambda^{87}Rb$ - 1.39 x 10^{-11} yr^{-1}) with an initial $^{87}Sr/^{86}Sr$ of 0.69937 ± 4 (Fig. 11), within error the same as other Apollo 15 mare basalts. The isochron is based on plagioclase, "ilmenite," and "cristobalite" separates, and both mechanical and density separation techniques were used.

Nakamura et al. (1977) studied the Sm-Nd isotopic system. Although Sm/Nd fractionations among separated phases were small, the data defined an isochron corresponding to 3.34 ± 0.09 b.y. ($\lambda^{147}Sm$ = 0.00654 x 10^{-9} yr^{-1}) with an initial $^{143}Nd/^{144}Nd$ of 0.50844 ± 0.00011. This age is consistent with the Rb-Sr age. Using the Moore County initial ratio, the source of 15065 was calculated to have $^{147}Sm/^{144}Nd$ of 0.1998 for a two-stage model, within the “chondritic” range of 0.195 ± 0.015.

TABLE 15065-2.

		,48	,29	,31	—	.32	—	,40	,33	,41	,37	,42	,39	,47	,126
Wt %	SiO2	43.30	48.66	48.47		47.24						48.2		49.0	
	TiO2	1.88	1.55	1.48		1.54			1.21			1.44		1.33	
	Al2O3	10.10	9.17	9.26		9.33			11.3			10.32		12.76	
	FeO	19.20	19.07	19.18		19.17			19.2			18.46		17.8	
	MgO	11.50	10.57	10.58		10.69						10.35		8.81	
	CaO	12.12	9.70	9.94		9.53						9.55		11.24	
	Na2O	0.715	0.36	0.34		0.23			0.282			0.33		0.3672	
	K2O	0.068	0.11	0.05	0.0464	0.05						0.041		0.0365,0.058	
	P2O5			0.05		0.08						0.104		0.062	0.076
(ppm)	Sc			38					41					39.1	
	V			158		185									
	Cr	5507	5600	3600		4400			4600			3200		3160	
	Mn	2300		2000		2000						1800		1890	
	Co	70		52		47			46	40				37.7	
	Ni	147		151		78		63							
	Rb			<1		5				0.39				0.70	
	Sr	214		110		98								134	
	Y			23		29								24	
	Zr			63		79								94	
	Nb			12		13								6	
	Hf								2.1					3.36	
	Ba			50		85								96	
	Th				0.51		0.5244							0.70	
	U				0.15		0.1368			0.085				0.190	0.14
	Pb						0.236								
	La			<10					5.1					7.73	
	Ce													20.6	
	Pr													3.15	
	Nd													14.6	
	Sm								3.4					4.72	
	Eu								0.94					1.14	
	Gd													5.3	
	Tb								0.7					0.96	
	Dy													6.66	
	Ho													1.2	
	Er													3.7	
	Tm														
	Yb			3.8					2.0					2.98	
	Lu								0.34					0.43	
	Li	7		5.9											6.7
	Be														
	B														
	C										12		11.2		
	N														
	S												600		
	F														40
	Cl														4.23a
	Br									8					12.2
	Cu	56		64		48								5.42	
	Zn	38						0.92		1.0				<1	
(ppb)	I														0.37
	At														
	Ga	24000		4100				3100						3760	
	Ge							21		6.7				<100	
	As													0.90	
	Se									53				80	
	Mo														
	Tc														
	Ru														
	Rh														
	Pd														
	Ag	5450								0.88					
	Cd							1.2		1.1					
	In							0.32		0.18					
	Sn														
	Sb									0.24					
	Te									0.96					
	Cs									23				50	
	Ta								400					450	
	W													102	
	Re									0.0094				<0.1	
	Os														
	Ir							0.048		0.144					
	Pt														
	Au	4						0.19		0.014				0.031	
	Hg														
	Tl									0.21					
	Bi									0.11					
		(1)	(2)	(3)	(4)	(5)	(6)	(7)	(8)	(9)	(10)	(11)	(12)	(13)	(14)

References and methods:

(1) Juan et al. (1972); AAS, colorimetric
(2) Longhi et al. (1972); microprobe fused bead
(3) Christian et al. (1972), Cuttitta et al. (1973); XRF, etc.
(4) O'Kelley et al. (1972); Gamma ray spectroscopy
(5) Strasheim et al. (1972); XRF, and others
(6) Tatsumoto et al. (1972); MS/ID
(7) Baedecker et al. (1973); RNAA
(8) Fruchter et al. (1973); INAA
(9) Ganapathy et al. (1973); GNAA
(10) Moore et al. (1973)
(11) Nava (1974); AAS, colorimetry, etc.
(12) Gibson et al. (1975); combustion, hydrolysis
(13) Wanke et al. (1975); XRF, RNAA, etc.
(14) Jovanovic and Reed (1976)

Note:

a = ril

TABLE 15065-3

		,8	,5	,6
Wt %	SiO2	47.95		47.7
	TiO2	2.30		2.86
	Al2O3	5.33		6.05
	FeO	23.60		23.77
	MgO	10.15		9.52
	CaO	9.30		9.33
	Na2O	0.25		0.27
	K2O	0.07		0.081
	P2O5	0.09		0.119
(ppm)	Sc	53		
	V	178		
	Cr	3400		3700
	Mn	2400		2400
	Co	66	45	
	Ni	54		
	Rb	1.0	0.76	
	Sr	100		
	Y	39		
	Zr	103		
	Nb	<10		
	Hf			
	Ba	75		
	Th			
	U		0.235	
	Pb			
	La	22		
	Ce			
	Pr			
	Nd			
	Sm			
	Eu			
	Gd			
	Tb			
	Dy			
	Ho			
	Er			
	Tm			
	Yb	6.6		
	Lu			
	Li	6.3		
	Be	<1		
	B	32		
	C			
	N			
	S			
	F			
	Cl			
	Br			
	Cu	14		
	Zn		1.6	
(ppb)	I			
	At			
	Ga	5300		
	Ge		5.3	
	As			
	Se		167	
	Mo			
	Tc			
	Ru			
	Rh			
	Pd			
	Ag		0.91	
	Cd		1.5	
	In		0.51	
	Sn			
	Sb		0.016	
	Te		3.4	
	Cs		60	
	Ta			
	W			
	Re		0.0015	
	Os			
	Ir		0.0054	
	Pt			
	Au		0.021	
	Hg			
	Tl		0.47	
	Bi		0.11	
		(3)	(9)	(11)

Unruh et al. (1984) reported Sm/Nd and Lu/Hf isotopic data for a whole-rock sample of 15065. The whole-rock values (Table 5) are similar to those for other Apollo 15 mare basalts, except that present day $\in$ Nd ($\in Nd_o$ in Table 5) is lower than olivine-normative basalt 15555. With the other analyzed quartz-normative mare basalt, 15076, it has the lowest $\in Nd_o$ among mare basalt groups except for the aluminous basalt 12038. Like all mare basalts, the Lu/Hf ratio is less than chondritic, thus $\in$ Hf has been falling since crystallization.

Strasheim et al. (1972) stated that the $^{7}Li/^{6}Li$ relationship gives an age of 3.30 b.y., but no information as to the derivation of this age is given. Rosholt (1972) discussed Th isotopes which contribute to radioactivity in the sample.

EXPOSURE AND TRACKS: Eldridge et al. (1972) reported cosmogenic radionuclide data: ^{22}Na and ^{26}Al have equilibrium values indicating a surface exposure of at least 2 m.y.

Bhattacharya et al. (1975) studied track densities for an interior chip. They did not provide specific data but bracketed the results with other rocks as a track density between 6 and 20 x $10^{6}/cm^{2}$, with an upper limit to the exposure (because no surface chip was studied) of 10-30 m.y.

TABLE 15065-4. Oxygen isotopes (°/oo, rel. SMOW) for mineral separates from 15065 (Clayton et al.)

Mineral	Plag	Pig	Cpx	Ilm	Trid
$\delta^{18}O$	5.84	5.60	5.47	4.08	6.72

TABLE 15065-5. Sm/Nd and Lu/Hf whole-rock data for 15065,137 (Unruh et al. 1984)

$^{147}Sm/^{144}Nd$	$(^{143}Nd/^{144}Nd)_o$	ϵNd_o	$(^{143}Nd/^{144}Nd)_I$	ϵNd_I	$^{176}Lu/^{177}Hf$	$(^{176}Hf/^{177}Hf)_o$	ϵHf_o	$(^{176}Hf/^{177}Hf)_I$	ϵHf_I
.1961±2	0.512723±22	+1.7±.4	0.50851±2	+2.0±.4	.02179±3	0.282481±74	-13.5±2.6	0.28106±7	+13.4±2.6

o = at present day; I = at time of crystallization

TABLE 15065-6. Elastic wave velocities (Km sec^{-1})
as a function of hydrostatic pressure (Chung, 1973)

Confining pressure in kilobars

	0.5	1.0	1.5	2	3	4	5	6	7
P	3.9	4.7	5.25	5.62	6.20	6.52	6.76	6.84	6.98
S	2.5	2.8	3.06	3.29	3.50	3.68	3.75	3.86	3.90

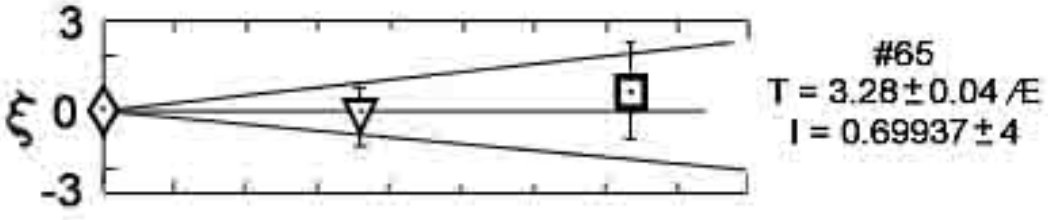

Figure 11. Deviations of mineral separates data from best fit isochron
(Papanastassiou and Wasserburg, 1973)

PHYSICAL PROPERTIES: Hargraves and Dorety (1972) reported NRM and its variation with alternating field demagnetization (Fig. 13) finding a weak remanence after demagnetization, similar to 15555.

Chung (1973) reported seismic wave velocities under confining pressures (Table 6) for sample ,27. Chung and Westphal (1973) reported dielectric spectra (Fig. 14) which are similar to 15555 and typical of gabbroic basalts.

Adams and McCord (1972) and Charrette and Adams (1975) reported diffuse reflection spectra (0.35 to 2.5 μm) for a powdered sample. The data show the preponderance of pigeonite as a slope in the 0.5 μm to 0.75 μm region steeper than the glassy vitrophyres.

PROCESSING AND SUBDIVISIONS: Prior to slabbing, the mafic segregation was chipped, providing ,2 from which thin sections ,87 and ,91 were made. From the same region ,3 and ,4 were chipped, and another several grams ground into a homogeneous powder and aliquotted into splits ,5 to ,11, some of which has not been allocated.

The "normal" rock was slabbed and the slab substantially dissected (Fig. 15). Several thin sections were made from ,24; ,25; and ,55. The large end piece (,0 in Fig. 15) was subsequently broken into smaller pieces along natural fractures; the two largest pieces are ,117 (575.6 g) in remote storage, and ,118 (544 g).

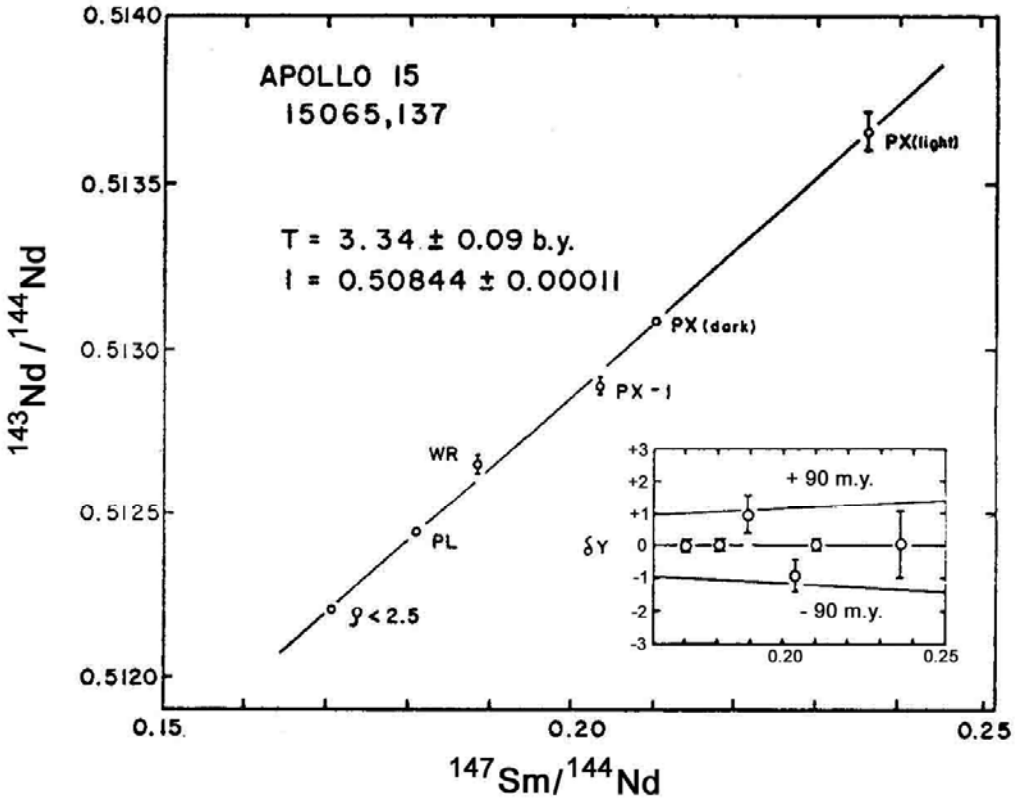

Sm-Nd evolution diagram for basalt 15065. The data are for "cristobalite" ($\rho < 2.5$), plagioclase ($\rho = 2.6$-2.8), whole rock, pyroxene + ilmenite ($\rho > 3.3$), hand-picked dark pyroxene (rim), and hand-picked light pyroxene (core) fractions. The data define a line which corresponds to a 3.34 ± 0.09 x 10^9yr age (2.77σ at 95% confidence). The whole rock and $\rho > 3.3$ fractions appear to deviate slightly from the line as can be seen in the δY (in 10^4) vs. X plot in the insert.

Figure 12. Sm-Nd internal isochron (Nakamura et al., 1977).

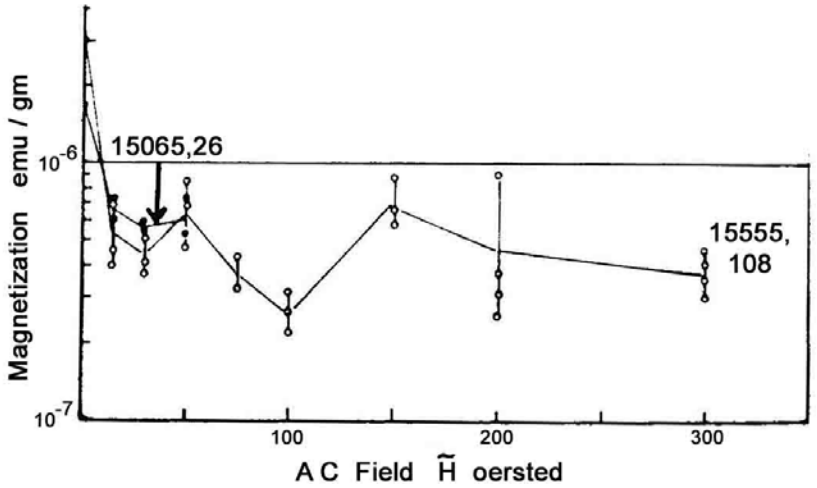

Figure 13. AF demagnetization (Hargraves and Dorety, 1972).

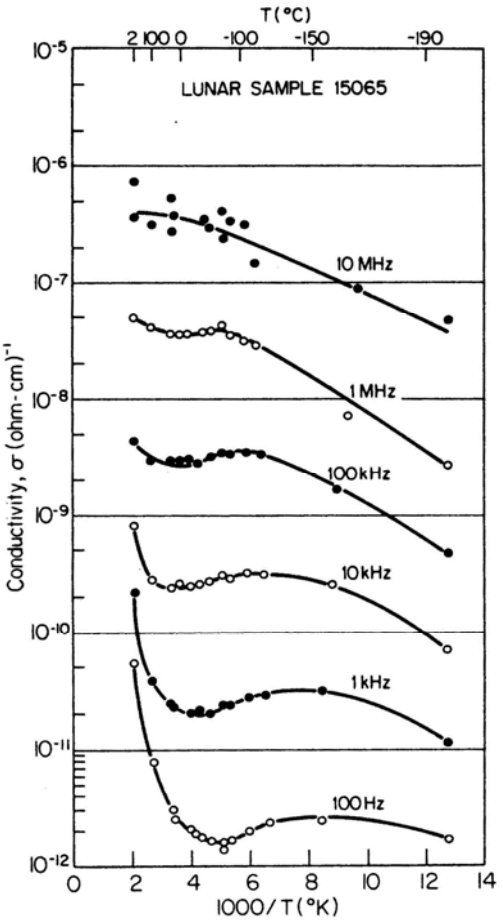

Electrical conductivity of sample 15065,27 as a function of frequency and temperature.

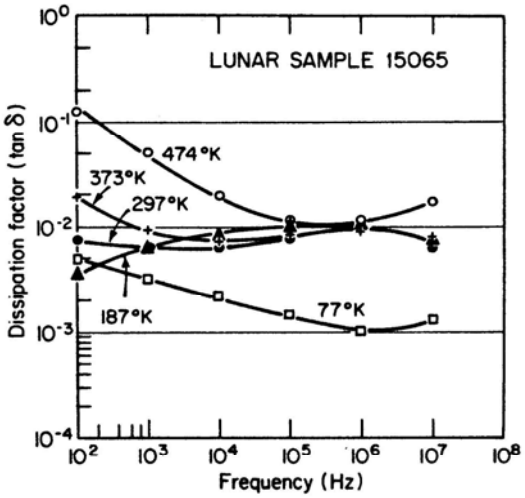

Dielectric losses in sample 15065,37 as a function of frequency and temperature.

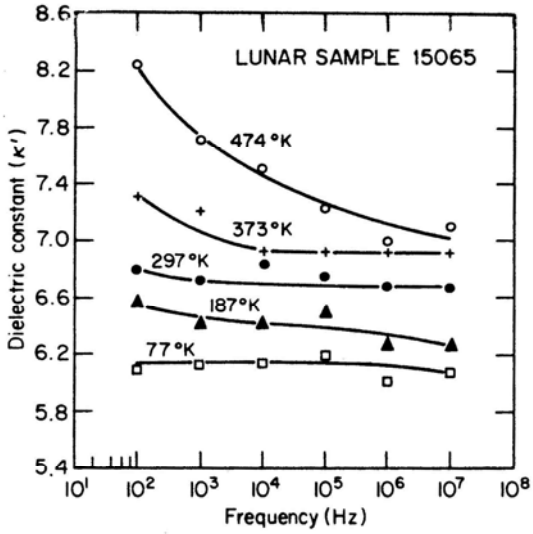

Dielectric constant of sample 15065,27 as a function of frequency and temperature.

Figure 14. Dielectric data (Chung and Westphal, 1973).

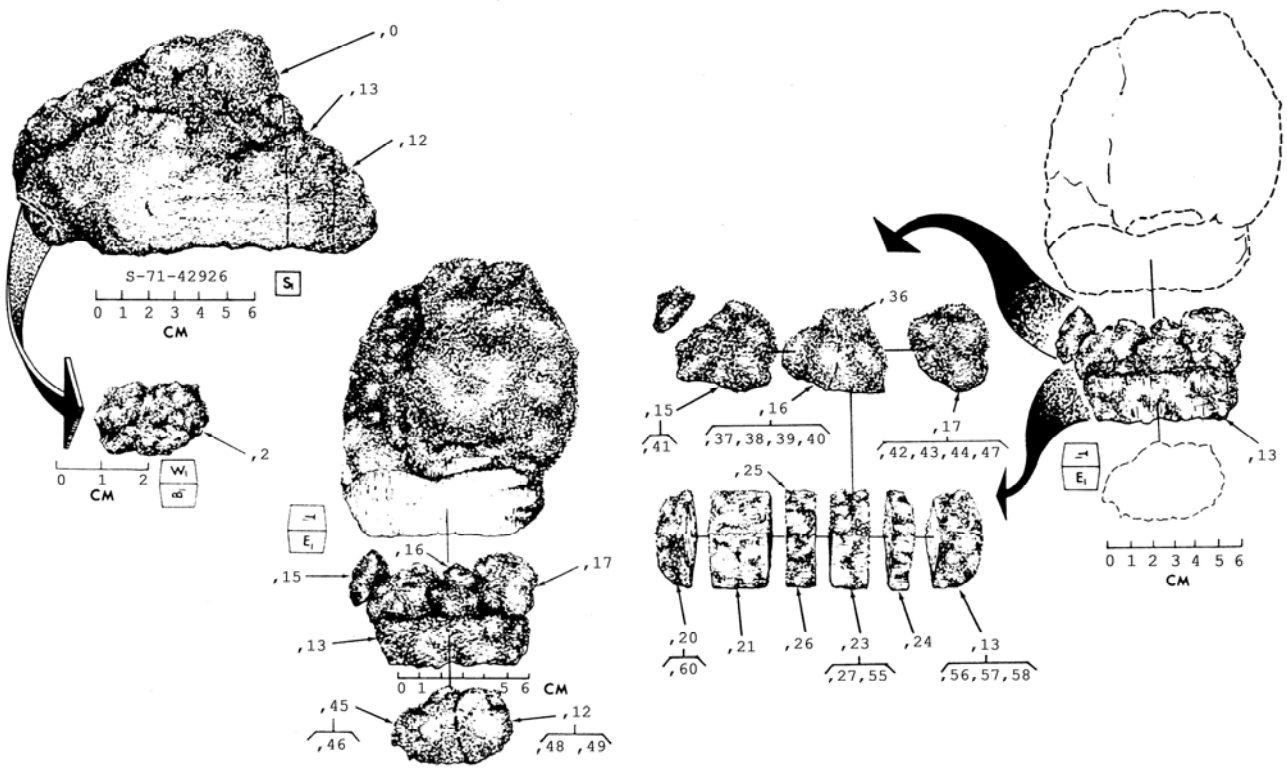

Figure 15. Main processing subdivisions.
Mafic segregation splits ,3 to ,11 not shown,
but are from same region as ,2.